ESTIMATION OF RUPTURE VELOCITY AND NEARFIELD Q FROM THE TABAS ACCELEROGRAMS OF THE SEPTEMBER 16, 1978, IRAN EARTHQUAKE

M. Niazi (I)
Presenting Author: M. Niazi

SUMMARY

Horizontal accelerograms of the September 16, 1978, Iranian earthquake (M_S = 7.4-7.7) recorded at Tabas are analyzed for the estimation of rupture velocity and nearfield Q. The derivations are based on the assumptions that the wave packet containing PGA is originated on the fault plane closest to the recording station and that the dynamic stress drop is nearly uniform over the rupture surface. The novelty of the method is in the utilization of a single recording station for the determination of important source and propagation parameters. An average rupture velocity close to 2.5 km/sec and mean $Q\beta$ of about 55 are obtained. While confirming the inferred pattern of rupture propagation, the particle motion rose diagrams indicate a multiple source character for the earthquake.

INTRODUCTION

The September 16, 1978, earthquake near Tabas, Iran, is the strongest earthquake (M_S = 7.4-7.7) of the instrumental era in that country. With a predominantly thrust mechanism (Ref. 1), this event was associated with 85 km of discontinuous faulting (Ref. 2). The earthquake resulted in total destruction of the town of Tabas and several of the satellite villages, and in a loss of over 15,000 lives. The main shock and several aftershocks were recorded by an SMA-1 accelerometer operating in Tabas (the main shock apparently triggered eight SMA-1 instruments operating over an epicentral distance range of about 200 km). One version of the digitized horizontal acceleration time histories for the main shock has already been subject to a preliminary analysis (Ref. 3). Here we use the same data with a slight modification to estimate the direction and average speed of the fault rupture. The only modification of the data resulted from the substitution of data for an approximately 0.5 second blank segment, three seconds in the transverse component record. The supplementary data were obtained from an alternative film copy on which the acceleration trace could be followed with some difficulty in this blank segment. The estimation of rupture velocity presented here is based on the assumption that the first long period pulse arriving right after the four second mark on the record is direct S phase radiated from the hypocenter where rupture initiated, and that the wave packet containing peak ground acceleration which arrives 5.5-6.0 seconds later would correspond to the passage of rupture closest to the recording station.

RUPTURE DIRECTION AND VELOCITY

The NEIS epicentral location and its relation to Tabas is shown in Figure 1. As such, the hypocenter is located near the southeastern end of the rupture zone, at an epicentral distance of about 50 km from Tabas. However, if the triggering of the accelerograph corresponds to the initial P-phase, as would be expected for

---

(I) Senior Geophysicist, TERA Corporation, Berkeley, California, USA

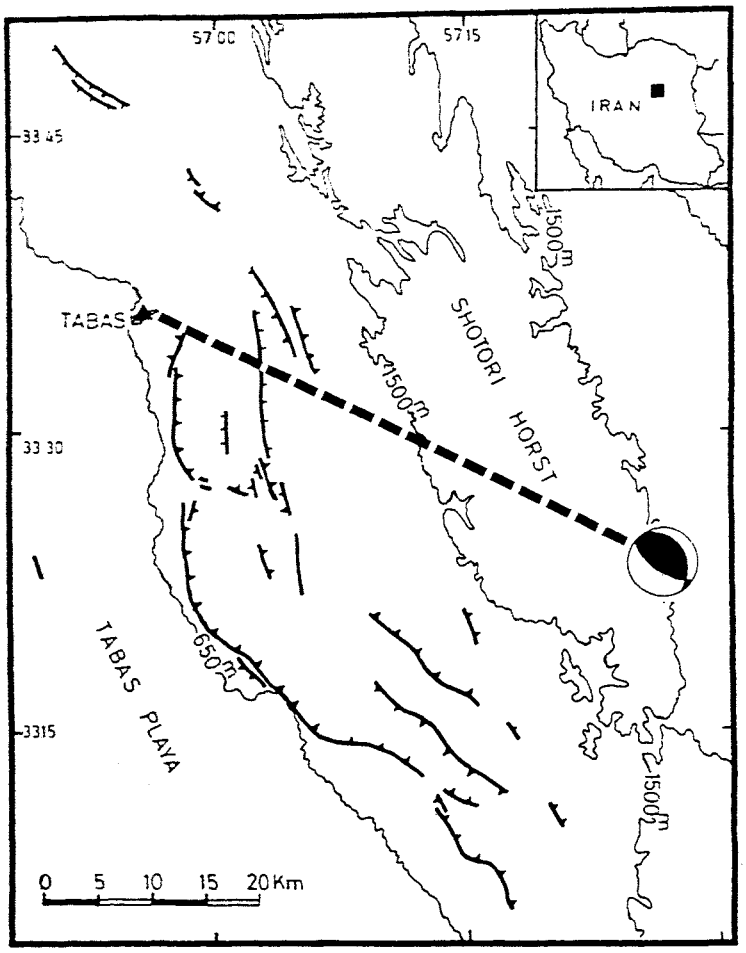

Figure 1 -- Topographic and fault map of the epicentral area, reproduced from Ref. 2. The discontinuous fresh surface fault traces, exhibiting predominantly thrust or reverse sense of motion, display a complex multiplanar pattern. The preferred fault plane solution of the mainshock (Ref. 1) is shown at the NEIS epicentral location. The NEIS epicentral distance of nearly 50 km, as represented by the length of the dashed line, may be overestimated by about 40%.

such a strong event, an epicentral distance of 30 km will be in better agreement with the 4.25 second S-P, assuming a midcrustal depth of 15 km. The NEIS estimated focal depth is normal (crustal). Therefore, regardless of the possibility of existence of a bilateral component, the northern limb of the rupture must have propagated towards Tabas on geometric grounds alone.

There is, however, independent confirmation of this northwestward progagation of rupture from consideration of the dominant directions of particle motion in the P-wave coda. Utilization of this technique has previously been applied to the study of source dynamics of the 1979 Imperial Valley earthquake by the author (Ref. 4). The main uncertainty in the application of the method to the Tabas records lies in the questions regarding the exact orientation of the instrument. In Figure 2 we have reproduced the initial 12 seconds of the Tabas horizontal records. The particle motion rose diagrams produced in the same figure for each consecutive second are derived on the assumption of north and east orientations of longitudinal and transverse components, respectively. The rose diagrams of Figure 2 clearly display a preferred counterclockwise rotation in agreement with the northward propagation of the rupture. If the shaded sectors were representing the rectilinear particle motion of the P wave radiated from the rupture front, they would indicate that the P wave initially approached Tabas mainly from an azimuth range of 120°-140°. The azimuthal ranges of the P wave approach in the following three seconds up to the S arrival are 110°-120°, 100°-110°, and 80°-90°, respectively. The described scenario is qualitative but can be used for the quantification of rupture velocity based on the known orientation of instruments. My indirect information indicates that the instrument was rotated about 15 degrees relative to N-S orientation; however, whether clockwise or counterclockwise is not known at this time. A +15° correction should be applied to the given azimuthal ranges if the instrument was installed in a counterclockwise rotated orientation, -15° otherwise.

As expected, the initial S wave particle motion is predominantly transverse to that of the initial P wave. Also, the particle motion diagrams predict additional sources, particularly in the 2-3 second interval of the record, which may be explained either by the bilateral character of rupture on a single fault plane, or multiple rupture planes as indicated by field observation. Niazi and Kanamori (Ref. 1) also cited probable departure of the fault plane from simple planar geometry for this earthquake in order to explain observed asymmetrical directivity in the farfield. In addition, 25 aftershocks with S-P time ranging from 0.7 seconds to 6.5 seconds have been recorded on the same film following the mainshock (Ref. 5).

A quantitative estimate of average rupture velocity may be obtained, if one assumes that the phase S_R containing the peak horizontal acceleration correspond ing to the S wave radiated from the closest approach of rupture to the station. When the observed 5.5 second delay of S_R relative to S is added to the estimated 10 second transition of S (for 30 km epicentral distance) and subtracted from the 3.5 second transition time for S_R, the rupture propagation time over the 30 km length of the fault will be $10.0 + 5.5 - 3.5 = 12.0$ sec. Therefore, the average rupture velocity V_R is derived from

$$V_R \simeq \frac{30}{12} = 2.5 \text{ km/sec}$$

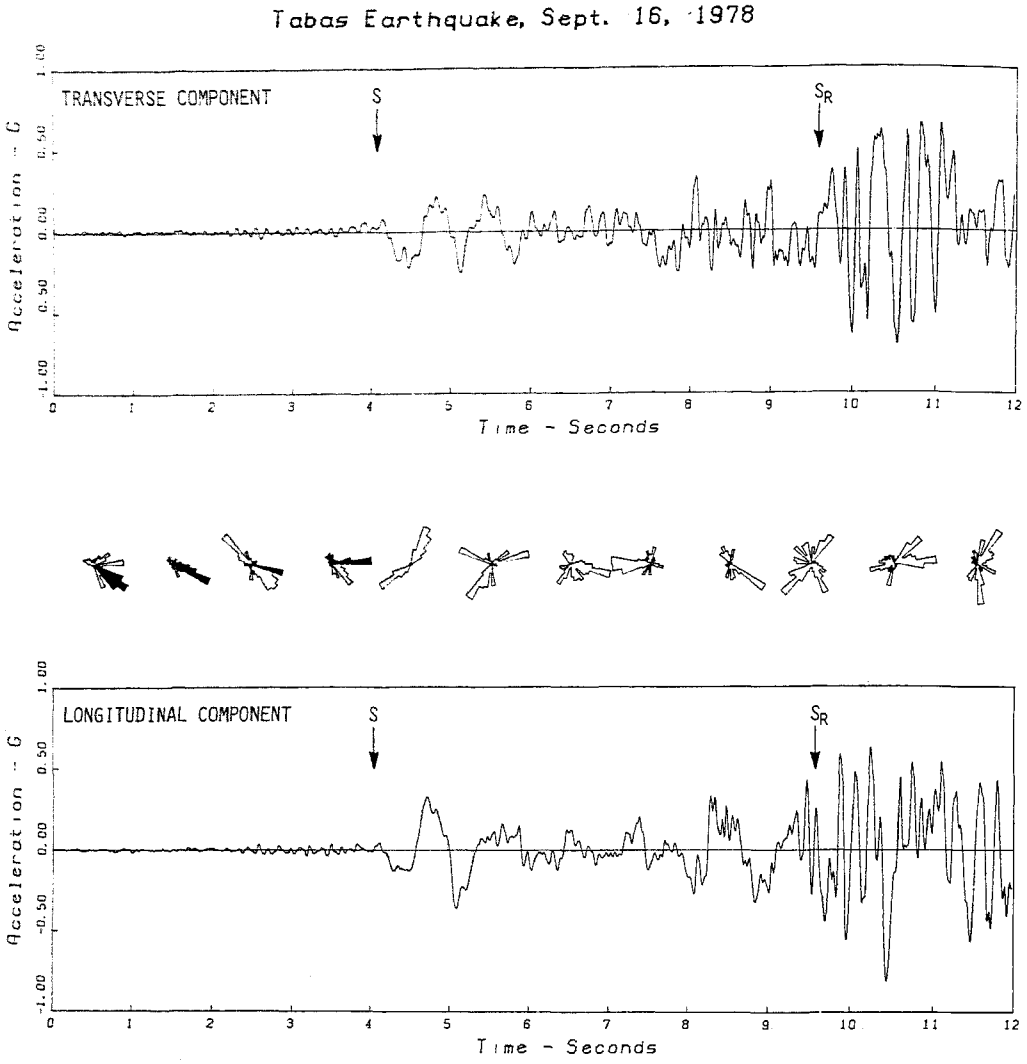

Figure 2 -- The first 12 seconds of the modified horizontal accelerograms of the main shock recorded at Tabas. S_R is assumed to have originated on the rupture surface closest to the station. The particle motion rose diagrams were computed (Ref. 4) under the assumption that upward motion of the longitudinal and transverse components correspond to the north and east directions, respectively. The counterclockwise rotation of the shaded sectors of the P coda implies a northward propagation of the rupture.

ESTIMATION OF Q IN THE NEARFIELD

Based on the assumptions of the preceding section, the spectra of S_R and S are compared for Q estimation. The selected windows on both components are 3.0-8.0 seconds for S and 8.0-13.0 seconds for S_R, as shown in Figure 3. The slope of spectral ratios of corresponding components within the frequency range of 1-5 Hz is taken to depend on the anelastic attenuation represented here by average Q. The effect of source geometry as expressed in the radiation pattern and geometrical spreading would only shift the ratio (Ref. 6). Comparable dynamic stress drop for the two source regions is, however, implicit in the method. Figure 3 shows the computed spectral ratios for each component.

Expressing the spectral ratios as $R(\omega)$,

$$R(\omega) = \frac{A'(\alpha, \omega)}{A(\alpha, \omega)} = K(\alpha) \left[e^{-\omega \int_{C'} \frac{ds}{QV}} - e^{-\omega \int_{C} \frac{ds}{QV}} \right]$$

then

$$\ln R(\omega) = \ln K(\alpha) - \omega \left[\int_{C'} \frac{ds}{QV} - \int_{C} \frac{ds}{QV} \right]$$

where $K(\alpha)$ represents the composite effect of the radiation pattern and geometrical spreading, and the second term on the right hand side reflects the differential anelastic attenuation of the two wave paths. The coefficient of $\omega = 2\pi f$ takes a very simple form when no spatial variation of Q is taken into account, in which case,

$$\ln R(\omega) = \ln K(\alpha) - \frac{2\pi f}{Q} (t' - t)$$

t and t' are the transit times of S and S_R, which for the assumed structure and focal depth are 10.0 and 3.5 seconds, respectively. Therefore, for the case of frequency independent Q, a simple relationship between the slope β of ln R vs. f and Q is derived for the Tabas fault zone, in the form of

$$\beta Q \simeq -41$$

The slope β of the spectral ratios, within the frequency range of 1 to 5 Hz, for the longitudinal and transverse components of acceleration are roughly -0.63 and -0.89 Hz^{-1}, respectively. The resulting shear wave Q from the two components are 65 and 46, with a mean value of 55. Figure 3 also shows that extension of the frequency range outside of 1-5 Hz is difficult due to noise introduced by the window length, application of low pass filter at 0.25 Hz cut-off frequency in the preprocessing, and possibly digitization noise (equispaced to 100 samples/sec in this study). It is further suggested that introduction of higher order terms may be required to explain the flattening of spectral ratios, indicating a breakdown of frequency independent Q assumptions for higher frequencies as has been observed in other regions of the world (Ref. 7, 8).

ACKNOWLEDGEMENTS

This study was partially supported by the National Science Foundation, Grant CEE-8213047. The technical support of Ann Bornstein is gratefully acknowledged.

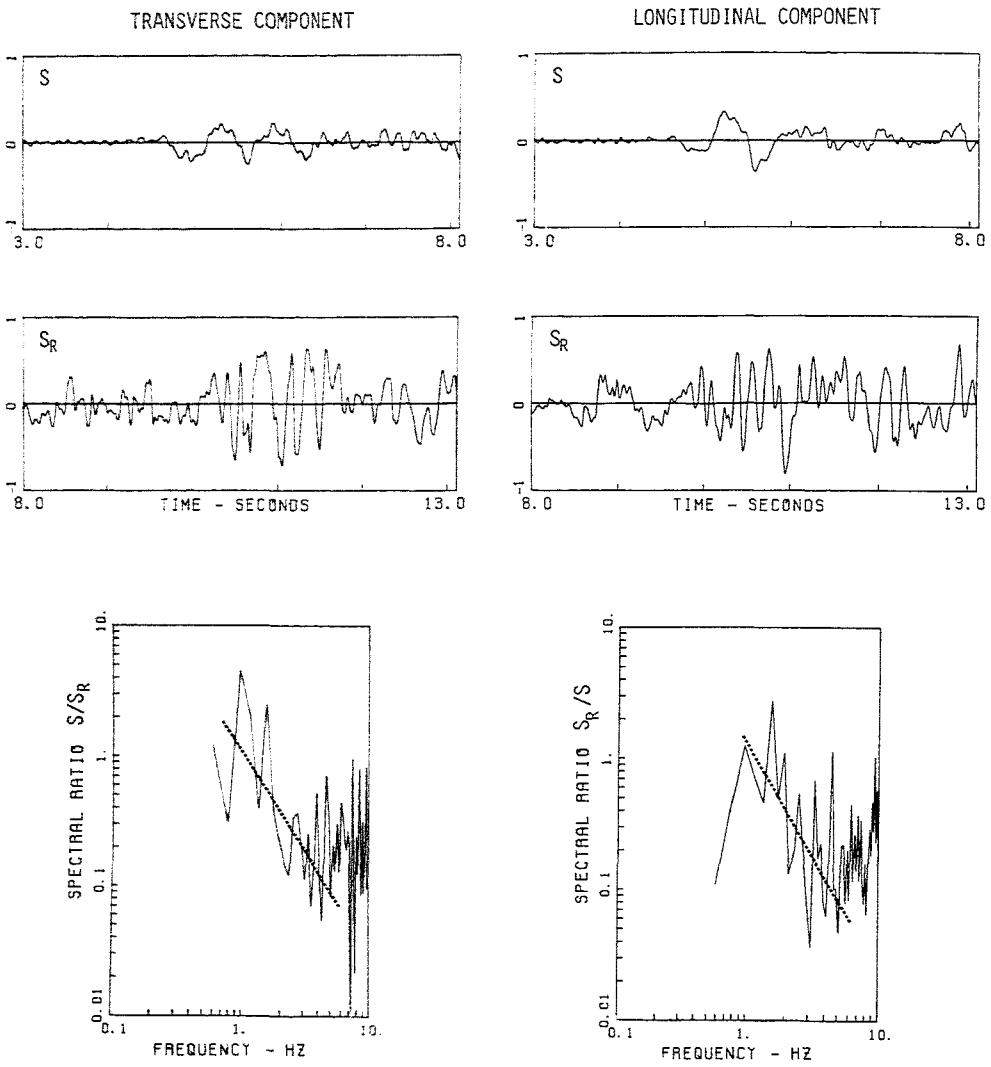

Figure 3 -- Spectral ratio of longitudinal and transverse components of S and S_R wave packets. The width of the time windows used in the spectral analysis is about 5 seconds.

REFERENCES

1. Niazi, M. and H. Kanamori, 1981, "Source Parameters of 1978 Tabas and 1979 Qainat, Iran, Earthquakes from Long-Period Surface Waves," Bulletin of the Seismological Society of America, 71, 1201-1213.

2. Berberian, M., I. Asudeh, R. G. Bilham, C. H. Scholz, and C. Soufleris, 1979, "Mechanism of the Main Shock and the Aftershock Study of Tabas-e-Golshan (Iran) Earthquake of September 16, 1978: A Preliminary Report," Bulletin of the Seismological Society of America, 69, 1851-1859.

3. Hadley, D. M., H. G. Hawkins, and K. L. Benuska, 1983, "Strong Ground Motion Record of the 16 September 1978 Tabas, Iran, Earthquake," Bulletin of the Seismological Society of America, 73, 315-320.

4. Niazi, M., 1982, "Source Dynamics of the 1979 Imperial Valley Earthquake from Near-Source Observations (of Ground Acceleration and Velocity)," Bulletin of the Seismological Society of America, 72, 1957-1968.

5. Ambraseys, N. N., 1983, Listing of the observed S-P readings of 25 aftershocks following the Tabas mainshock, personal communication.

6. Niazi, M., 1971, "Seismic Dissipation in Deep Seismic Zones from the Spectral Ratio of pP/P," Journal of Geophysical Research, 76, 3337-3343.

7. Apsel, R. J., S. K. Singh, J. C. Fried, and J. N. Brune, 1982, "Spectral Attenuation of SH Waves Along the Imperial Fault," Bulletin of the Seismological Society of America, 72, 2003-2016.

8. Rovelli, A., 1982, "On the Frequency Dependence of Q in Friuli from Short Period Digital Records," Bulletin of the Seismological Society of America, 72, 2369-2372.